The asymmetry of female meiosis reduces the frequency of inheritance of unpaired chromosomes

Daniel Cortes[1], Karen McNally[1], Paul E. Mains[2] and Francis J. McNally[1,3]

1. Department of Molecular and Cellular Biology
149 Briggs Hall
University of California, Davis
Davis, CA 95616
USA

2. Department of Biochemistry and Molecular Biology
University of Calgary
Calgary, Alberta TN2 4N1
CANADA

3. Corresponding author
Francis J. McNally
Department of Molecular and Cellular Biology
149 Briggs Hall
University of California, Davis
Davis, CA 95616
phone: (530)754-8018
FAX: (530)752-3085
email: fjmcnally@ucdavis.edu

running head: elimination of univalents

Abbreviations: FISH: fluorescence in situ hybridization, XXX: trisomy for the X chromosome

SUMMARY

Trisomy, the presence of a third copy of one chromosome, is deleterious and results in inviable or defective progeny if passed through the germ line. Random segregation of an extra chromosome is predicted to result in a high frequency of trisomic offspring from a trisomic parent. *C. elegans* with trisomy of the X chromosome, however, have far fewer trisomic offspring than expected. We found that the extra X chromosome was preferentially eliminated during anaphase I of female meiosis. We utilized a mutant with a specific defect in pairing of the X chromosome as a model to investigate the apparent bias against univalent inheritance. First, univalents lagged during anaphase I and their movement was biased toward the cortex and future polar body. Second, late-lagging univalents were frequently captured by the ingressing polar body contractile ring. The asymmetry of female meiosis can thus partially correct pre-existing trisomy.

Introduction

During female meiosis, a G2 oocyte containing four genome copies undergoes two asymmetric cell divisions depositing one genome in a single haploid egg while the other three genomes are segregated into polar bodies. These divisions are mediated by meiotic spindles that are asymmetrically positioned against the oocyte cortex with the pole-to-pole axis of the spindle perpendicular to the cortex. Both the inheritance of only one of four genome copies and the distinct perpendicular positioning of the meiotic spindle are remarkably conserved among animal phyla suggesting a selective advantage (Fabritius et al., 2011a; Maddox et al., 2012; Maro and Verlhac, 2002).

Several advantages of asymmetric meiosis have been suggested previously, yet none are applicable to all animals. Asymmetric meiotic spindle positioning maximizes the volume of a single egg, helps prevent interference with the meiotic spindle by the sperm aster (McNally et al., 2012), and preserves predetermined embryonic polarity gradients. Here we suggest a previously unrecognized advantage of asymmetric meiosis, the ability of meiotic spindles to correct trisomy by preferentially depositing the extra chromosome copy into a polar body.

Accurate segregation of homologous chromosomes to opposite spindle poles depends on a physical attachment, or chiasma, between homologous chromosomes. A chiasma consists of a crossover, which holds the two homologous chromosomes together in a bivalent so that kinetochores can be properly oriented towards opposite poles (Miller et al., 2013; Moore and Orr-

Weaver, 1998). When a chiasma does not form, univalent chromosomes may maintain sister cohesion and move to poles independent of their homologs at anaphase I as can occur in *S. cerevisiae* (Buonomo et al., 2000). If a univalent chromosome biorients, loses cohesion, and segregates sister chromatids at anaphase I (eg. Kouznetsova et al., 2007; LeMaire-Adkins and Hunt, 2000; Nicklas and Jones, 1977), the resulting single chromatid will segregate randomly at anaphase II. Random segregation of homologs at anaphase I or single chromatids at anaphase II should result in equal frequencies of haplo and diplo ova in the case of a trisomy (Fig. 1A), and equal frequencies of nullo and diplo ova in the case of a crossover failure.

Deviations from random segregation are suggested by observations of X chromosomes in *Caenorhabditis elegans*. In *C. elegans*, the single unpaired X chromosome from an XXX mother is inherited with unexpectedly low frequency with twice as many haploX ova produced as diploX ova (Hodgkin et al., 1979). HIM-8 is a zinc finger protein that binds to specific DNA sequences that are enriched on the X chromosome. *him-8* mutants have a pairing defect that is completely specific for the X chromosome, resulting in two X univalents and 5 autosomal bivalents in 95% of diakinesis oocytes (Phillips et al., 2005). If the two X univalents segregated randomly, *him-8* mutants would be expected to produce equal frequencies of nulloX ova and diploX ova. However, Hodgkin et al. (1979) demonstrated a 5-fold preponderance of nulloX ova over diploX ova in *him-8*. Using sex-reversed *him-8* XX males, these authors showed the oposite effect in spermatogenesis. Rather than producing the 50% haploX, 25% diploX, 25%

nulloX sperm expected from random segregation, *him-8* XX males produced 86% haploX, 3% diploX, 11% nullo X sperm, indicating symmetric distribution of univalents during male meiosis. Thus achiasmate maternal X chromosomes are inherited with unexpectedly low frequency in worms.

Five mechanisms might reduce the frequency of trisomic offspring from trisomic or *him-8* mothers. First, trisomic embryos might die during embryonic development resulting in undercounting of XXX offspring. This is unlikely in *C. elegans* because both XXX and *him-8* mutant mothers produce a very low frequency of dead embryos (Hodgkin et al., 1979; Supplementary File 1). A second possibility is that mitotic non-disjunction in the XXX mother results in a mosaic gonad that contains both diploX and triploX oocytes. Selective apoptosis of XXX germline cells (Bhalla and Dernburg, 2005) would then enrich for XX germline cells. This does not contribute to the segregation bias in *C. elegans* as the most mature diakinesis oocytes in *him-8* and wild-type XXX worms have 7 rather than 6 DAPI-staining bodies (Phillips et al., 2005; this study). A third possibility is that a univalent present during metaphase I or a single chromatid present during metaphase II would be broken or otherwise degraded during anaphase. A fourth possibility is that many XXX progeny look normal because of the stochastic nature of dosage compensation and thus are undercounted. A fifth possibility is that univalent chromosomes present at metaphase I are preferentially placed in the first polar body. Here we demonstrate that indeed, biased deposition of univalent X chromosomes into the first polar body reduces

129 the frequency of trisomic zygotes resulting from oocytes with unpaired X
130 chromosomes.
131
132
133

Results

XXX wild-type oocytes preferentially lose the achiasmate X chromosome between metaphase I and metaphase II

Elimination of the extra chromosome from an oocyte starting with a trisomy would result in rescue to a euploid state. It has previously been shown that *C. elegans* XXX wild-type oocytes have a paired bivalent X and an unpaired univalent X chromosome in pachytene (Goldstein, 1984). We picked wild-type XXX adult hermaphrodites from the progeny of an XXX strain (AV494, Mlynarczyk-Evans *et al.*, 2013) based on their characteristic dumpy morphology as described by Hodgkin et al. (1979). Meiotic embryos from XXX mothers were fixed and stained for microtubules and DNA. Chromosomes are well separated by bundles of microtubules during *C. elegans* female meiotic metaphase. This unique morphology facilitates counting of individual chromosomes on the metaphase plate when viewed down the pole to pole axis of the spindle (Fig. 1B). We found that 100% of metaphase I meiotic embryos from XXX wild-type worms had 7 DAPI-staining bodies on the spindle [Fig 1C, F], consistent with 6 bivalents and a single univalent X. Two chromosomes were labelled with an X-specific fluorescence in situ hybridization (FISH) probe in these spindles (Fig. 1C, Supplementary file 2). This result shows that a mosaic gonad resulting from mitotic nondisjunction cannot explain the low frequency of XXX offspring from XXX worms. If the univalent segregated randomly during anaphase I, 50% of metaphase II spindles should have 6 DAPI-staining bodies (6 bivalents) and 50% should have 7 DAPI-staining bodies (6 bivalents and one univalent). Instead,

71% of metaphase II spindles contained only 6 DAPI-staining bodies and only 29% contained 7 DAPI-staining bodies [Fig 1D-F]. These frequencies match the 2:1 ratio of X to XX ova previously interpreted from genetic studies (Hodgkin et al., 1979) and are significantly different than the 50% expected from random segregation (one tailed p= 0.004, Pearson's Chi Squared test). This result eliminates the possibilities that XXX mothers have many XXX offspring that are undercounted due to incomplete penetrance of the XXX dumpy phenotype, or that hermaphrodite nulloX sperm contribute significantly to the low frequency of XXX self progeny. The finding that all assayed metaphase I spindles had 7 chromosomes also indicates that our method of identifying XXX worms as dumpy individuals is accurate and the high frequency of metaphase II spindles with 6 chromosomes is not a result of misidentifying diploid worms as XXX worms. FISH with an X-specific probe revealed that in 6/6 metaphase II embryos with only 6 DAPI-staining bodies, a single hybridization signal was present in the spindle and 2-3 hybridization signals were present in the polar body (Fig. 1D; Supplementary file 3). Because only a single X-hybridization signal was observed in the first polar body in 5/5 spindles from diploids, these results demonstrate that single X univalents are deposited in the first polar body with greater than 50% frequency.

X and V univalents are frequently deposited in the first polar body

To further investigate the mechanism leading to preferential loss of univalents during meiosis I, we utilized *him-8* worms as a more tractable model. It has previously been shown that diakinesis stage *him-8* oocytes have 5

autosomal bivalents and two X univalents (Phillips et al., 2005). If segregation of the two X univalents was random, these worms should produce equal numbers of nullo X and diploX ova. Instead, *him*-8 mutants produce a 5-fold higher frequency of nulloX ova over diploX ova (Hodgkin et al., 1979), indicating that both maternal X univalents are lost at some time after diakinesis in a large fraction of embryos. To determine when maternal X univalents are preferentially lost, we imaged both live embryos within *him-8* worms expressing GFP::tubulin and mCherry::histone (Fig. 2A-E) and also fixed embryos stained with DAPI and anti-tubulin antibodies (Fig. 2F-J). We assayed the number of chromosomes (defined here as DAPI-staining or mCherry:histone-positive bodies that would include univalents and bivalents) present at metaphase of meiosis I and II (Fig. 2K). At meiosis I metaphase, 7 chromosomes were present in 96% of *him-8* embryos [Fig 2B, K], with the remainder having 6 chromosomes. If the two univalents segregated randomly without losing cohesion, 25% of metaphase II spindles would be expected to have 5 autosomes and no X, 50% would have 5 autosomes and 1 X and 25% would 5 autosomes and 2 X chromosomes. Instead, 40% of *him-8* metaphase II embryos had 5 chromosomes, 55% had 6 chromosomes and only 5% had 7 chromosomes [Fig 2K]. These frequencies differ significantly from those expected from unbiased segregation (Chi-square test, two tailed $p < 0.0001$), closely match the ratio of nulloX to diploX ova inferred by Hodgkin et al. (1979), and support the hypothesis that the majority of X univalents are eliminated between metaphase I and metaphase II. These

maternal chromosome counts are also unaffected by nullo X or diplo X sperm that might contribute to phenotype-based progeny counts.

To confirm that the two chromosomes lost between these stages were indeed the X univalents, we used fluorescence in situ hybridization (FISH) with a lac operator probe to detect a multicopy lac operator array integrated on the X chromosomes in a *him-8* background [Fig 2F-J]. FISH revealed two X univalents and 7 total DAPI-staining bodies on 93% of all the *him-8* metaphase I plates (Fig. 2G, L). At metaphase II, FISH revealed at least two X hybridization foci in the first polar body and none on the metaphase plate when the spindle had 5 DAPI-staining bodies (Fig 2H). When 6 DAPI-staining bodies were present on the metaphase II plate, we always observed one X hybridization focus each on the metaphase plate and in the first polar body (Fig 2I). Finally, metaphase II embryos containing 7 DAPI-staining bodies had two X hybridization foci on the metaphase plate and none in the first polar body [Fig 2J]. Together, these results demonstrate that both achiasmate X univalents are deposited into the first polar body in 40% of *him-8* embryos as compared with the 25% expected from random segregation.

To test whether achiasmate autosomes are also placed in the first polar body with higher than random frequency, we analyzed a strain with a Lac operator array integrated on chromosome V and bearing a loss of function mutation in the *him-8* homolog *zim-2*, which contributes to chromosome V pairing (Phillips and Dernburg, 2006). Unlike the situation with *him-8* and pairing of the X, redundancy between ZIM proteins may contribute to chromosome V pairing.

Phillips and Dernburg reported only 72% of diakinesis oocytes with 7 rather than 6 DAPI-staining bodies in a *zim-2* mutant and our *zim-2* strain with lacO(V) had only 62% of diakinesis oocytes with 7 DAPI-staining bodies (Figure 2- figure supplement 1 F). FISH revealed two distinct chromosome V hybridization foci and 7 DAPI-staining bodies on 41% of metaphase I spindles (Figure 2- figure supplement 1 A, E). Starting with 41% achiasmate V's, random segregation should yield 10% of metaphase II embryos with both V's in the first polar body (25% of 41%). Instead, FISH revealed 27% of metaphase II embryos had five DAPI-staining bodies on the metaphase plate and chromosome V hybridization foci only in the first polar body (Figure 2- figure supplement 1 B, E). Likewise, random segregation of achiasmate V's should yield 10% metaphase II spindles with 7 DAPI-staining bodies on the metaphase II spindle, two distinct chromosome V hybridization foci on the spindle and none in the first polar body. Only 5% of this embryo class was observed (Figure 2- figure supplement 1 D, E). These frequencies are significantly different than those expected from random segregation (Chi-square test, two tailed $p<0.0002$). The discrepancy in the fraction of *zim-2* oocytes with 7 DAPI-staining bodies at diakinesis versus metaphase I raises the possibility that chromosomes might be systematically undercounted in *zim-2* metaphase I spindles (but not in wild-type, *him-8* or XXX metaphase I spindles). If this is the case, the two V univalents must be positioned close together on the spindle because 0/57 *zim-2* metaphase I plates with 6 DAPI-staining bodies had two widely spaced lacO(V) FISH foci and the deviation between expected and observed nulloV metaphase II spindles would

be even greater. Two results strongly indicate that the same mechanisms acting on univalent X's in *him-8* mutants also act on V univalents in the *zim-2* mutant. First, the 5-fold preponderance of metaphase II spindles with 5 DAPI-staining bodies over those with 7 DAPI-staining bodies is similar to *him-8*. Second, the presence of lacO FISH signal only in the first polar body of metaphase II embryos with 5 DAPI-staining bodies on the spindle is the same in *him-8* and *zim-2*. Thus achiasmate autosomes, like achiasmate X chromosomes, are preferentially deposited into the first polar body.

Univalents biorient at metaphase I and tend to lag during anaphase I

To understand the mechanism by which univalent X chromosomes are preferentially deposited in polar bodies, we examined their orientation and position in the spindle. Antibodies specific for the cohesin subunit, REC-8, label a cruciform on metaphase I bivalents (Fig 3A, B), and a single band on metaphase II chromosomes (Fig 3A, C). The single REC-8 bands on wild-type metaphase II chromosomes and on *him-8* metaphase I univalents were both oriented perpendicular to the pole to pole axis of the spindle (Fig 3D), indicating that *him-8* X univalents biorient at metaphase I. *him*-8 worms expressing GFP::KNL-2, which labels the *C. elegans* cup-shaped meiotic kinetochores (Dumont et al., 2010), were also analyzed for biorientation and yielded the same conclusion as analysis by REC-8 antibody (Figure 3 - figure supplement 1). We also examined the localization of GFP:AIR-2, the aurora B kinase that is essential for loss of cohesion at anaphase I and which is loaded between homologs of wild-type bivalents in a chiasma-dependent fashion (Rogers et al.,

2002). The fluorescence intensity of GFP::AIR-2 was 2.3 times higher on bivalents than univalents at metaphase I of *him-8* embryos (Figure 3 - figure supplement 2 B,C). AIR-2 is normally re-loaded between sister chromatids at metaphase II. GFP::AIR-2 on metaphase II chromosomes was 1.7 times higher than on *him-8* metaphase I univalents (Figure 3 - figure supplement 2 C) indicating that the reduced amount of AIR-2 on metaphase I univalents was not simply a consequence of the smaller size of a univalent relative to a bivalent. AIR-2 is required for the crossover-dependent, prometaphase, partial removal of REC-8 from between homologs in a wild-type bivalent, an event proposed to be essential for loss of cohesion at anaphase I (Severson and Meyer, 2014). Consistent with the low levels of AIR-2, *him-8* univalents had 1.7 +/- 0.3 times the intensity of REC-8 staining as the inter-homolog region of bivalents in the same spindle (Fig. 3B; n=8 embryos, two tailed p = .04 Chi Square relative to expected 1.0).

Because X univalents biorient at metaphase I but load half as much AIR-2, which is required for loss of cohesion at anaphase I in *C. elegans* (Kaitna et al., 2002; Rogers et al., 2002), and retain twice as much REC-8, we hypothesized that bioriented univalents might be pulled toward both spindle poles and lag on the anaphase spindle as they fail to lose cohesion. To test this possibility, we did time-lapse imaging of *him-8* embryos expressing GFP::tubulin and mCherry::histone, focusing specifically on the events of anaphase I. 90% of *him-8* embryos at anaphase I had one or two lagging chromosomes (n=119), compared to 2% of wild-type embryos (n=52) [Fig 4A, B]. In 51% of living *him-8*

295 embryos with lagging chromosomes at anaphase I, two discrete lagging
296 chromosomes could be resolved. Each lagging chromosome eventually moved
297 as a single unit either toward the cortex or into the embryo in 98% of embryos (n
298 = 179) (Fig. 4B, 5A) indicating that cohesion between sister chromatids is
299 maintained and that univalents are not broken or destroyed during anaphase. At
300 anaphase II, only 10% of *him-8* embryos exhibited lagging chromosomes (n=60)
301 and 0/22 wild-type embryos had lagging chromosomes, suggesting that lagging
302 chromosomes are caused by the presence of univalents at meiosis I.
303 To confirm that the lagging chromosomes are bioriented X univalents, we
304 used LacO(X) FISH. We found that the X-specific FISH probe labeled one or two
305 lagging chromosomes at anaphase I of *him-8* embryos, indicating that lagging
306 chromosomes are X univalents (13/14) (Fig. 4D). 36% of fixed *him-8* anaphase I
307 embryos with lagging chromosomes had two distinct FISH positive chromosomes
308 lagging. Another 21% had a single FISH-positive lagging body but no other FISH
309 positive chromosomes on the spindle indicating that the two X univalents were
310 likely too close to resolve in these embryos. The remaining 36% had one FISH
311 positive lagging chromosome and one FISH positive chromosome in one of the
312 main chromosome masses (one embryo had a lagging chromosome that was a
313 bivalent). These results suggest that one or both X univalents lag in up to 90% of
314 *him-8* embryos.
315 Similar results were obtained for chromosome V in *zim-2* mutants, where
316 40% of metaphase I embryos have univalent V's (Figure 2 - figure supplement 1).
317 27% (4/15 or over half of anaphase I spindles expected to have V univalents)

had a lagging chromosome. 100% (4/4) of these lagging chromosomes were chromosome V as assayed by LacO(V) FISH (Fig 4E). These results indicate that achiasmate autosomes lag at anaphase I, just like achiasmate X chromosomes.

The meiotic contractile ring captures lagging X univalents in the first polar body

After establishing that lagging chromosomes were univalents, we next asked if univalents that lagged were subject to biased segregation at anaphase I. To analyze this we conducted time-lapse imaging of embryos from *him-8* worms expressing GFP::tubulin and mCherry::histone as well as embryos from *him-8* worms expressing these along with GFP::PH (plextrin homology domain) to label the plasma membrane (Fig 5A). Our time-lapse analysis revealed that 65% of lagging chromosomes eventually moved toward the cortex and the forming polar body of *him-8* embryos during anaphase I (n= 181) (Fig 5B), indicating that preferential expulsion of lagging univalents into the first polar body could contribute to the higher than random frequency of metaphase II spindles with 5 autosomes and no X. Because the polar body contractile ring ingresses inward toward the midpoint of the late anaphase spindle where it normally scissions, we hypothesized that the preferential resolution of lagging chromosomes toward the cortex might result from inhibition of contractile ring scission until the ring ingresses past lagging chromosomes (Fig 5C). In wild type, ingression of the

polar body contractile ring initiates when homologs have separated by 2.3 μm and polar body scission completes when homologs have separated by 5.6 μm (Fabritius et al., 2011b). The bias of univalents that moved toward the cortex before initiation of contractile ring ingression could not be caused by engulfment by the polar body. Therefore we separated lagging univalents into two categories, early resolving univalents that moved to one pole while the main chromosome masses were separated by less than 4.0 μm and late resolving univalents that moved to one pole only after the main chromosome masses were separated by greater than 4.0 μm. If late resolving univalents were engulfed during polar body formation, elimination of contractile ring activity would reduce the fraction of lagging chromosomes resolving toward the cortex. Indeed, RNAi depletion of the non-muscle myosin, NMY-2, which causes complete loss of cortical furrowing and polar body formation (Fabritius et al., 2011b), in *him-8* embryos resulted in a significant ($p = .02$) reduction in the percentage of late lagging univalents resolving toward the cortex from 64% to 43% (Fig. 5B).

As a complementary approach, we asked if more rapid polar body ring ingression would have the opposite effect of NMY-2 depletion. We previously showed that depletion of the myosin phosphatase, MEL-11, doubled the rate of polar body ring ingression (Fabritius et al., 2011b). Therefore we hypothesized that inactivation of MEL-11 might enhance the preferential engulfment of lagging univalents by the first polar body. Unlike NMY-2 depletion which generates 100% dead embryos, the lethality of *mel-11* mutants is rescued by wild-type sperm so the chromosome constitution of progeny from a *mel-11* mother can be

364 scored by phenotype. Mating otherwise wild-type males bearing the recessive X-
365 linked marker, *lon-2*, to *him-8* hermaphrodites allows measurement of the
366 frequency of nullo X ova (which give rise to lon male progeny) and diplo X ova
367 (which give rise to XXX dumpy progeny) (Hodgkin et al., 1979). Random
368 segregation of univalents should generate a 1:1 ratio of nullo X:diplo X ova. We
369 found that *mel-11* increased the segregation bias of *him-8* by 7-fold from 3:1 to
370 23:1 (Table 1). This result indicates that more rapid furrow ingression captures
371 more lagging univalents in the first polar body resulting in more nulloX ova.
372 To test our hypothesis that a lagging chromosome inhibits contractile ring
373 scission to allow univalent capture, we asked whether the presence of late
374 lagging univalents might cause misplacement of the contractile ring from the 50%
375 spindle length scission point observed in wild-type embryos (Fabritius et al.,
376 2011b) by time-lapse imaging of the plasma membrane marker GFP::PH (Fig.
377 5A). Spindle length was measured between the outside edges of the main
378 chromosome masses and only in frames in which both chromosome masses
379 were in focus (Fig. 5C). In *him-8* embryos, when there were no lagging
380 univalents, the contractile ring ingressed normally to 50% spindle length as
381 measured from the outside edge of the main chromatin mass in the interior of the
382 embryo. When a lagging univalent was seen segregating into the polar body, the
383 contractile ring was seen ingressing deeper into the embryo to 40% spindle
384 length (Fig. 5C, D). Alternatively, when a lagging univalent was seen
385 segregating into the embryo, the contractile ring ingressed inward to a shallower
386 depth at 59% spindle length (Fig. 5C, D).

To further test the idea that a late-lagging univalent might influence the choice of the scission point, we imaged formation of the first polar body in wild-type or *him-8* worms expressing GFP:UNC-59 (septin) and mCherry: histone. Septins are polymerizing GTPases that assemble in the contractile ring with myosin II, F-actin and anillins (Green et al., 2013). In wild type or *him-8* with early resolving univalents, GFP:UNC-59 labeled a flat washer-shaped contractile ring that moved down to the midpoint of the elongating anaphase spindle as reported previously for GFP:NMY-2 (Fabritius et al., 2011b). The septin ring transformed into a tube (Fig. 6A, 255 sec) as previously described for myosin and ANI-1 (Dorn et al., 2010). When cortical furrowing relaxed at the end of telophase I, the septin tube moved outward to the embryo surface, then flopped over and remained as a separate entity next to the chromosomes in the first polar body (Fig. 6A, 420 sec). In 5/10 *him-8* embryos in which the septin-labeled ring reached the lagging univalent, the univalent was trapped in the septin tube and moved with the septin tube outward during cortical relaxation (Fig. 6B). In these cases, the univalent remained trapped in the septin tube adjacent to the polar body as shown in Fig. 6B and C. In 3/10 cases, the septin ring passed the univalent before the tube was formed and in these cases the univalent joined the main mass of chromatin in the polar body. In the 2/10 cases where the univalent did not end up in the polar body, the univalent slipped out of the septin tube into the embryo before the septin tube moved toward the embryo surface. These results are consistent with a model where the septin tube traps late-lagging univalents until scission occurs on the embryo side of the septin tube.

To further test the idea that late-lagging univalents are physically trapped in the septin tube, we tried to influence the integrity of the septin tube without blocking polar body scission. Septins act together with anillins (Green et al., 2013). *C. elegans* has three anillins: ANI-1 which is required for polar body scission, ANI-2 which is required for gonad development and ANI-3 which has no known function (Maddox et al., 2005). We hypothesized that ANI-3 might play a non-essential structural role in the polar body septin tube and that *ani-3(RNAi)* might therefore allow late-lagging univalents to slip out of the tube back into the embryo. Indeed RNAi of ANI-3 initiated on L4 *him-8* hermaphrodites (which have already completed spermatogenesis) significantly ($p<0.001$ binomial test) reduced the fraction of XO male progeny from 37% (n= 9 mothers, 1960 progeny) to 27% (n = 11 mothers, 2123 progeny) whereas *ani-3 (RNAi)* had no significant effect on wild -type worms (wt: 0.04% XO, 1% dead, n= 11 mothers; *ani-3 (RNAi)*: 0.05% XO, 1% dead, n = 17 mothers). This result suggests that compromising the integrity of the septin tube may reduce the efficiency of trapping lagging univalents in the septin tube. ANI-3 depletion did not significantly increase the frequency of XXX dumpy progeny from *him-8* mothers (*him-8*: 3% XXX, 5% dead; *him-8 ani-3(RNAi)*: 4% XXX, 6% dead). This apparent inconsistency might be explained if additional ANI-3-independent mechanisms act to reduce the number of XXX progeny (see below).

The early anaphase segregation bias

Lagging chromosomes were resolved prior to contractile ring ingression in 45% of embryos with lagging chromosomes at anaphase I. These were resolved toward the cortex 64% of the time (n=72) and NMY-2 depletion had no significant effect on this class of embryos (p = .8) (Fig. 5B). These results suggest that an additional mechanism biasing univalent movement toward the cortex might be at work earlier in the cell cycle. During wild-type meiosis, bivalents congress to the metaphase plate on an 8 μm long spindle that is oriented parallel to the cortex. Upon anaphase promoting complex activation, the meiosis I spindle shortens to 4.8 μm in length (Yang et al., 2003), then one spindle pole moves to the cortex in a dynein-dependent manner and homolog separation initiates (Ellefson and McNally, 2009, 2011). We found that univalents were misaligned toward the spindle poles in fixed *him-8* embryos at late metaphase I, when the meiotic spindle is shortened but not yet rotated (Fig. 7A-B). In 46% of these embryos, both univalents were misaligned toward the same pole (Fig. 7B), close to the 50% expected from random positioning. In fixed *him-8* embryos at the onset of anaphase, when spindles are shortened and rotated, but chromosomes are not yet separated, 57% had one or both univalents closer to the cortical pole (38 + 19%; Fig. 7F,G). No embryos had both univalents closer to the interior spindle pole. We hypothesized that one of two mechanisms might link spindle rotation with the early anaphase preference for univalent movement toward the cortex. Univalents might stochastically align closer to one spindle pole before rotation and bias the movement of that pole to

the cortex. Alternatively, the cortex-proximal pole might acquire distinct biochemical properties after rotation due to cortical contact and subsequently generate more pulling force on the lagging univalents and pull them preferentially toward the cortex.

To test whether spindle rotation is involved with the *him-8* segregation bias, we utilized *mei-2(ct98)*, a partial loss of function katanin mutant which causes a failure of meiotic spindle rotation but still allows polar body formation and production of viable progeny (McNally et al., 2006). If offset univalents bias spindle rotation or if the cortex-proximal pole exerts greater pulling on univalents after rotation, then a *mei-2(ct98) him-8* double mutant should have a reduced frequency of male progeny relative to *him-8* alone. At 20°C the *mei-2(ct98) him-8* double mutant produced only 21% male progeny (n = 1440 progeny from 14 parents) which is significantly less than the 36% male progeny produced by the *him-8* single mutant (n = 964 progeny from 8 parents; $p < 0.0001$ by one-tailed binomial test) and is significantly different than *mei-2 (ct98)* alone (0% males; n = 925 progeny from 8 parents). The reduction in male progeny is unlikely to be due to effects on spermatogenesis as sperm is unaffected by katanin null mutants (Mains et al., 1990). This result is consistent with either spindle rotation based models for the early anaphase segregation bias. The role of spindle rotation is not conclusive, however, since *mei-2(ct98)* meiotic spindles have other phenotypes besides spindle rotation failure (McNally et al., 2006).

Absolute distinction between the two possible rotation models would require unambiguous tracking of both univalents before during and after spindle

rotation. This was not possible in any of 201 time-lapse sequences. In 8 particularly clear time-lapse sequences, one or both univalents could be identified unambiguously 10 - 100 seconds before initiation of spindle rotation. In 6/8 of these cases, the univalent-proximal pole rotated to the cortex (Fig. 7I, H). In 1/8 cases, the univalent-proximal pole rotated away from the cortex. In 1/8 cases, the 2 univalents were offset to opposite poles both before and during rotation. If the cortical environment conferred a stronger pulling force on the cortical pole after rotation, then lagging univalents crossing the midpoint of the anaphase spindle should be common. Time-lapse imaging of spindles after rotation revealed that among 30 embryos in which one or two lagging chromosomes were already positioned closer to one pole at anaphase I onset and the lagging chromosome resolved early, the lagging chromosome resolved toward the pole that it was already close to in 80% of these embryos (data not shown). Among the 20% of embryos in which the lagging chromosome moved to the opposite pole after spindle rotation, the chromosome moved toward the cortex 3 times, toward the embryo 3 times, and in one instance, the two lagging chromosomes resolved to opposite poles. These observations are not consistent with a cortical pole that generates a stronger pulling force after rotation but instead favor the idea that the offset position of univalents before rotation increases the probability that the univalent-proximal pole will move to the cortex.

Two results suggested that additional factors might contribute to the overall inheritance of univalent X chromosomes. Both *ani-3(RNAi)* and *mei-2(ct98)* reduced the frequency of male self progeny from *him-8* worms without

increasing the frequency of triploX self progeny. We therefore tested whether aneuploid sperm might influence phenotypic outcomes by LacO(X) FISH on pronuclear stage embryos from self-fertilized *him-8* mothers (not shown). Before pronuclear meeting, male pronuclei are distinguished from female pronuclei by the presence of sperm asters. We observed 90% haploX, 8% nulloX and 2% diploX male pronuclei (n = 52). These values are significantly different than the 50%, 25%, 25% expected from random segregation (two tailed p<.0001 by Chi Square) and are similar to the frequencies obtained by Hodgkin et al. (1979) using genetic tests with sex reversed *him-8* XX males. 10% nulloX sperm thus make a small contribution to reducing the frequency of XXX self progeny.

Discussion

Hodgkin et al. (1979) showed that *C. elegans* that are trisomic for the X chromosome or that fail to form a chiasma between the normal two X homologs, have fewer trisomic offspring than expected from random segregation. Our results explain this phenomenon by demonstrating that two cellular pathways preferentially segregate X univalents into the first polar body. Mechanisms reducing the frequency of trisomic offspring have not been investigated in other model organisms because in both mouse and *Drosophila*, animals with trisomy X are not fertile (Tada et al., 1993; Schupbach et al., 1978) and there are no mutants, like *him-8*, that specifically block crossover formation on one specific chromosome in females. However, women with trisomy 21 or trisomy X are often fertile and have been reported to have more than 50% euploid offspring (Bovicelli et al., 1982; Neri, 1984; Ratcliff et al., 1991; Robinson et al., 1991; Stewart et al., 1991). Triploid oysters provide a stronger example of apparent female-specific correction to a diploid state. Eggs produced by triploid females and fertilized with sperm from diploid males result in 57% diploid, 31% triploid and 12% aneuploid offspring whereas eggs produced by diploids and fertilized by sperm from triploids result in 15% diploid and 85% aneuploid offspring (Gong et al., 2004). Gauging the liklihood that the phenomenon described here for *C. elegans* might be relevant to trisomic humans or triploid oysters is complicated by two issues. In contrast with trisomic *C. elegans*, triploid oysters (Guo and Allen, 1994) and trisomic human oocytes sometimes form trivalent structures rather than a separate bivalent and univalent. Only 42 - 16% of diplotene oocytes from

fetuses with trisomy 21, trisomy 13 or trisomy 18 exhibited a separate bivalent and univalent (Robles et al., 2007; Roig et al., 2005). It is difficult to predict the behavior of trivalents on the spindle. In addition, it is not clear whether a univalent present during anaphase I of a human or oyster oocyte would be more likely to move to one pole intact as in *C. elegans* or to separate equationally. We speculate that single chromatids resulting from equational separation of univalents at anaphase I could be subjected to asymmetric segregation at anaphase II. Our results suggest that any chromosome that lags during late anaphase might be prefentially expelled simply due to the conserved, asymmetric nature of polar body formation.

There is one example where a univalent chromosome exhibits the opposite of the segregation bias reported here in *C. elegans*. In the 44 - 78% of oocytes from XO mice in which the univalent segregates intact at anaphase I, the univalent is preferentially retained in the embryo (Lemaire-Adkins and Hunt, 2000). This appears to be a difference between worms and mice rather than a difference between a trisomy and a monosomy since sex-reversed XO *C. elegans* produce an excess of nulloX ova (Hodgkin, 1980).

Discerning the overall significance of preferentially placing univalents into the first polar body is a complex problem. In the case of an XXX mother or a mother with a mosaic ovary containing trisomic and diploid oocytes, these pathways would increase the frequency of normal haploid eggs relative to that expected from random distribution of a single univalent (Fig. 1). In the case of diploid oocytes with two univalent autosomes, however, 100% efficient expulsion

of univalents into the first polar body would increase the frequency of lethal monosomy. Data shown in Fig. 2, however, show no significant decrease in haploid eggs (interpreted from the frequency of MII spindles with 6 chromosomes) from *him-8* or *zim-2* mothers relative to the 50% that would occur by random distribution. Thus the efficiency of placing univalents in the first polar body has evolved to a point that corrects trisomy without reducing the frequency of haploid eggs produced from oocytes that failed to form a chiasma between one pair of homologs. The conservation of these mechanisms in other species will have to be elucidated by studies focused specifically on the concept of chromosomal errors that are corrected, rather than caused, by female meiotic spindles.

Experimental Procedures

Worm strains

The genotypes of *C. elegans* strains used in this work are listed in Supplementary File 1. For LacO(X) FISH, EG7477, which has Lac operator arrays integrated on chromosome II and X was outcrossed to *him-8* males or to wild-type males to eliminate the extra LacO array on chromosome II, generating strains FM299 (wild-type LacO(X)) and FM300 (*him-8* lacO(X)). The loss of the chromosome II LacO array and homozygosity for the X chromosome array were confirmed by PCR.

RNAi

RNAi was carried out by feeding bacteria (HT115) induced to express double-stranded RNA (Timmons et al., 2001). The clones used were *nmy-2* I-3L24, *ani-3* V-12J23 (Kamath et al., 2001).

Live imaging

Adult hermaphrodites were anesthetized with tricaine and tetramisole and immobilized between a coverslip and agarose pad on a slide. The time-lapse images shown in Fig. 2A-E and 4A-B were captured on an Olympus IX71 microscope equipped with a 60x PlanApo NA 1.42 oil objective and an ORCA R2 CCD camera (Hamamatsu Photonics). Hg arc excitation light was shuttered by a Sutter Lambda 10-3 shutter controller (Sutter Instruments). Images shown in Fig. 5A were captured with an Intelligent Imaging Innovations Marianas Spinning Disk Confocal equipped with a Photometrics Cascade QuantEM 512SC EMCCD, and

Zeiss 63X 1.4 objective. Image sequences in Fig. 6 were captured with a Perkin Elmer-Cetus Ultraview Spinning Disk Confocal equipped with an Orca R2 CCD and an Olympus 60X 1.4 objective.

Immunofluorescence

Meiotic embryos were extruded from hermaphrodites by gentle squishing between coverslip and slide, flash frozen in liquid N2, permeabilized by removing the coverslip, then fixed in cold methanol before staining with antibodies and DAPI. Antibodies used in this work were mouse monoclonal anti-tubulin (DM1alpha) (Sigma) [1:200], mouse monoclonal DM1alpha:FITC conjugated (Sigma) [1:30], rabbit anti-REC-8 (from Josef Loidl) [1:500], Alexa 594 anti-rabbit and Alexa594 anti-mouse (both from Molecular Probes and used at 1:200). Images in Fig. 3 were captured with an Applied Precision Deltavision Deconvolution system equipped with an Olympus PlanApo 60X 1.40 objective and a CoolSnap HQ CCD camera (Photometrics). Deltavision Z-stacks were captured at 130nm intervals. Images in Fig. 1, 2A'-E', 4C-E, 7, and S1 were captured with the Olympus IX71 described above but using an Olympus DSU (disc scanning unit). Z stacks were acquired by taking images every 200 nm (unless otherwise noted) from the top to the bottom of the spindle tubulin signal.

Deconvolution

Deconvolution was performed on most images shown. Deconvolution of time-lapse movies from the IX71 was performed using Huygens Professional X11 (Scientific Volume Imaging) with PSFs determined from bead images.

Deltavision Z-stacks were deconvolved using Softworx native deconvolution software with PSFs calculated from bead images taken on that system.

IF-C-FISH: Immunofluorescence with chromosome fluorescence in situ hybridization

A lac operator oligonucleotide CCACATGTGGAATTGTG AGCGGATAACAATTTGTGG and an oligonucleotide corresponding to an X-specific repeat, XC (Phillips et al., 2005) TTTCGCTTAGAGCGATTCCTTACCCTTAAATGGGCGCCGG, were each synthesized with 3' and 5' Texas Red and used in hybridization to LacO arrays integrated on X or V or to endogenous X sequences. FISH with immunofluorescence was performed as described by Phillips et al. (2009) with some modifications.

Worms were washed in 0.8% egg buffer and then placed on slides pre-coated with poly-L-lysine (Sigma). Worms were then gently crushed between the slide and a 25mm sq. #1 coverslip to extrude meiotic embryos and immediately submerged in liquid nitrogen for 10-15 minutes. Coverslips were then flicked off to freeze-crack eggshells, and slides were submerged in -20°C methanol for 20-30 minutes. Slides were then washed in 1X PBS twice for 10 minutes and then in 1X PBST (0.2% Tween-20) for 10 minutes. Slides were then blocked in 1X PBST with 4% BSA for 30-45 minutes at room temperature in a moist chamber. Blocking solution was wicked away being careful not to dry out the samples and FITC-conjugated DM1a was applied 1:30 in 1X PBST with 4% BSA using 20 µL

coverwells (Grace BioLabs). Slides were incubated in this antibody for 4 hours at room temperature or left overnight at 4°C. Slides were then washed sequentially in 1X PBST, 1X PBS, and 2X SSCT (0.4% Tween-20) for 10 minutes each. Following the last wash, slides underwent secondary fixation in 7% formaldehyde in 1X egg buffer for 5 minutes and were immediately dipped in 2X SSCT to wash off fixative. Slides were then washed in 2X SSCT twice for 5 minutes each and then pre-hybridized. Pre-hybridization was performed by adding 200 µL of 50% formamide in 2X SSCT with a 200 µL coverwell (Grace BioLabs) overnight at 37°C in a moist chamber. After 24 hours, slides were taken out of 37°C incubation and placed at room temperature while the FISH probe was prepared. The FISH probe was prepared by adding 0.6 µL of the stock [900ng/uL] to 30uL of hybridization buffer (hybridization buffer was made as described in Phillips et al., 2009) with 300 µL/mL salmon sperm DNA and 0.1% Tween-20 per slide. Slides were then incubated in 30 µL of this solution under a hybridization slip (Grace BioLabs) at 95°C for 3 minutes on an OmniSlide (Thermo Scientific) and then at 37°C in a moist chamber for 48-72 hr. Following this incubation slides were washed in 50% formamide in 2X SSCT as before but for 2 one hour incubations. Finally slides were stained with DAPI by submerging in a Coplin jar filled with 2X SSCT 6 µg/ml DAPI for 10 minutes, and were then washed for 30 minutes in fresh 2X SSCT. Slides were then wicked dry with a Kimwipe taking care not to dry out the sample and were mounted with 8 µL of DABCO Mowiol and sealed with nail polish. Following 2-3 days for curing, slides were imaged.

Metaphase chromosome counts

Chromosome counts were carried out on live embryos in utero or on fixed embryos extruded from the worm by locating metaphase spindles whose chromosomes were all aligned at the metaphase plate. Z stacks were captured at 200nm intervals. Spindles that were oriented sideways, with their metaphase plates perpendicular to the imaging plane, were reconstructed using ImageJ 3D stack reconstruction and chromosomes were counted only if individual masses could be discerned. Metaphase II spindles were distinguished from metaphase I spindles by the presence of polar bodies.

Analysis of lagging chromosome resolution

Time lapse images of lagging chromosomes in FM125, FM126 and FM232 were acquired at 10 s intervals beginning at late metaphase I when the spindle is shortening and rotating and continuing through polar body extrusion and the formation of the metaphase II spindle. The direction of resolution was determined from the last frame where the lagging chromosome was still discernable from the segregating chromosome masses. At this frame, spindle length was determined by measuring the distance between the outside edges of the main masses of segregating chromosomes. Lagging chromosomes that decided which way to go when the spindle was more than 4 μm long were classified as late resolving because earlier work indicated that myosin dependent polar body scission occurs when spindles are longer than 4 μm (Fabritius et al., 2011b). We confirmed this assumption by finding that 5/5 FM232 (GFP:PH) spindles longer than 4 μm exhibited deep cortical furrows.

For *nmy-2(RNAi)* time-lapse sequences, only embryos in which polar body extrusion completely failed were analyzed. The fate of lagging chromosomes was scored based on whether they ended up at the cortex or in the interior prior to the formation of the metaphase II spindle. Often, chromosomes at the cortex were picked up by the metaphase II spindle. These were still scored as cortex fated lagging chromosomes.

Acknowledgements

We thank the following for *C. elegans* strains: Christian Frøkjær-Jensen, Erik Jorgensen, Aaron Severson, Barbara Meyer, Anne Villeneuve, Amy Maddox, Becky Green, Karen Oegema, Paula Checci and the Caenorhabditis Genetics Center, which is funded by the NIH Office of Research Infrastructure Programs (P40 OD010440). This work was supported by National Institute of General Medical Sciences Grant 1R01GM-079421 (to F.J.M.), a grant from the Canadian Institutes of Health Research (To P.E.M.), a fellowship from the Floyd and Mary Schwall (to D.C.) and NIH training grant T32 GM007377 (to D.C). We also thank Dan Starr, JoAnne Engebrecht, Amy Fabritius, Lesilee Rose and Jon Flynn for critical reading of the manuscript.

715

716

717 **References**

718

719 Bhalla, N., and Dernburg, A.F. (2005). A conserved checkpoint monitors meiotic
720 chromosome synapsis in Caenorhabditis elegans. Science *310*, 1683-1686.

721

722 Bovicelli, L., Orsini, L.F., Rizzo, N., Montacuti, V., and Bacchetta, M. (1982).
723 Reproduction in Down syndrome. Obstet. Gynecol. 59(6 Suppl):13S-7S.

724

725 Buonomo, S.B., Clyne, R.K., Fuchs, J., Loidl, J., Uhlmann, F., and Nasmyth, K.
726 (2000). Disjunction of homologous chromosomes in meiosis I depends on
727 proteolytic cleavage of the meiotic cohesin Rec8 by separin. Cell *103*, 387-398.

728

729 Checchi, P.M., Lawrence, K.S., Van, M.V., Larson, B.J., Engebrecht, J. 2014.
730 Pseudosynapsis and Decreased Stringency of Meiotic Repair Pathway Choice
731 on the Hemizygous Sex Chromosome of Caenorhabditis elegans Males.
732 Genetics. 197: 543-560.

733

734 Dorn, J.F., Zhang, L., Paradis, V., Edoh-Bedi, D., Jusu, S., Maddox, P.S., and
735 Maddox, A.S. (2010). Actomyosin tube formation in polar body cytokinesis
736 requires Anillin in C. elegans. Curr Biol *20*, 2046-2051.

737

738 Dumont, J., Oegema, K., and Desai, A. (2010). A kinetochore-independent
739 mechanism drives anaphase chromosome separation during acentrosomal
740 meiosis. Nat. Cell Biol. *12*, 894-901.
741
742 Ellefson, M.L., and McNally, F.J. (2009). Kinesin-1 and cytoplasmic dynein act
743 sequentially to move the meiotic spindle to the oocyte cortex in Caenorhabditis
744 elegans. Mol. Biol. Cell *20*, 2722-2730.
745
746 Ellefson, M.L., and McNally, F.J. (2011). CDK-1 inhibits meiotic spindle
747 shortening and dynein-dependent spindle rotation in C. elegans. J. Cell Biol. *193*,
748 1229-1244.
749
750 Fabritius, A.S., Ellefson, M.L., and McNally, F.J. (2011a). Nuclear and spindle
751 positioning during oocyte meiosis. Curr. Opin. Cell Biol. *23*, 78-84.
752
753 Fabritius, A.S., Flynn, J.R., and McNally, F.J. (2011b). Initial diameter of the polar
754 body contractile ring is minimized by the centralspindlin complex. Dev Biol *359*,
755 137-148.
756
757 Frøkjær-Jensen, C., Davis, M.W., Sarov, M., Taylor, J., Flibotte, S., LaBella, M.,
758 Pozniakovsky, A, Moerman, D.G., and Jorgensen, E.M. 2014. Random and
759 targeted transgene insertion in *Caenorhabditis elegans* using a modified Mos1
760 transposon. Nat Methods. 11: 529-534.

761

762 Goldstein, P. (1984). Triplo-X hermaphrodite of *Caenorhabditis elegans*:
763 pachytene karyotype analysis, synaptonemal complexes, and pairing
764 mechanisms. Canadian Journal of Genetics and Cytology *26*, 13-17.

765

766 Gong, N., Yang, H., Zhang, G., Landau, B.J., and Guo, X. (2004). Chromosome
767 inheritance in triploid Pacific oyster Crassostrea gigas Thunberg. Heredity
768 (Edinb). 93: 408-415.

769

770 Green, R.A., Mayers, J.R., Wang, S., Lewellyn, L., Desai, A., Audhya, A., and
771 Oegema, K. (2013). The midbody ring scaffolds the abscission machinery in the
772 absence of midbody microtubules. J. Cell Biol. *203*, 505-520.

773

774 Guo, X., and Allen, S.K. (1994). Reproductive potential and genetics of triploid
775 pacific oysters, Crassostrea gigas (Thunberg). Biol. Bull. 187: 309-318.

776

777 Hodgkin, J. (1980). More sex-determination mutants of *Caenorhabditis elegans*.
778 Genetics. *96*, 649-664.

779

780 Hodgkin, J., Horvitz, H.R., and Brenner, S. (1979). Nondisjunction Mutants of the
781 Nematode *Caenorhabditis elegans*. Genetics *91*, 67-94.

782

783 Kaitna, S., Pasierbek, P., Jantsch, M., Loidl, J., and Glotzer, M. (2002). The
784 aurora B kinase AIR-2 regulates kinetochores during mitosis and is required for
785 separation of homologous chromosomes during meiosis. Curr. Biol. *12*, 798-812.
786
787 Kamath, R.S., Martinez-Campos, M., Zipperlen, P., Fraser, A.G., and Ahringer, J.
788 (2001). Effectiveness of specific RNA-mediated interference through ingested
789 double-stranded RNA in Caenorhabditis elegans. Genome Biol. *2*,
790 RESEARCH0002.
791
792 Kemphues, K.J., Kusch, M., Wolf, N. (1988). Maternal-effect lethal mutations on
793 linkage group II of *Caenorhabditis elegans*. Genetics. 120: 977-986.
794
795 Kouznetsova, A., Lister, L., Nordenskjöld, M., Herbert, M., Höög C. (2007). Bi-
796 orientation of achiasmatic chromosomes in meiosis I oocytes contributes to
797 aneuploidy in mice. Nat. Genet. *39*, 966-968.
798
799 Lemaire-Adkins, R. and Hunt. P. (2000). Nonrandom segregation of the mouse
800 univalent X chromosome: evidence of spindle-mediated meiotic drive. Genetics
801 *156*, 775-783.
802
803 Lewellyn, L., Carvalho, A., Desai, A., Maddox, A.S., Oegema, K. (2011). The
804 chromosomal passenger complex and centralspindlin independently contribute to
805 contractile ring assembly. J. Cell Biol. 193: 155-169.

Maddox, A.S., Habermann, B., Desai, A., and Oegema, K. (2005). Distinct roles for two *C. elegans* anillins in the gonad and early embryo. Development. *132*, 2837-2848.

Maddox, A.S., Azoury, J., and Dumont, J. (2012). Polar body cytokinesis. Cytoskeleton *69*, 855-868.

Maro, B., and Verlhac, M.H. (2002). Polar body formation: new rules for asymmetric divisions. Nat. Cell Biol. *4*, E281-283.

McNally, K.L., Fabritius, A.S., Ellefson, M.L., Flynn, J.R., Milan, J.A., and McNally, F.J. (2012). Kinesin-1 prevents capture of the oocyte meiotic spindle by the sperm aster. Dev. Cell *22*, 788-798.

McNally, K., Audhya, A., Oegema, K. and McNally, F.J. (2006). Katanin controls mitotic and meiotic spindle length. J. Cell Biol. *175*, 881-891.

Miller, M.P., Amon, A., and Unal, E. (2013). Meiosis I: when chromosomes undergo extreme makeover. Curr. Opin. Cell Biol. *25*, 687-696.

Moore, D.P., and Orr-Weaver, T.L. (1998). Chromosome segregation during meiosis: building an unambivalent bivalent. Curr. Top. Dev. Biol. *37*, 263-299.

Mlynarczyk-Evans, S., Roelens, B., and Villeneuve, A.M. (2013). Evidence that masking of synapsis imperfections counterbalances quality control to promote efficient meiosis. PLoS Genet. *9*, e1003963.

Neri, G. (1984). A possible explanation for the low incidence of gonosomal aneuploidy among the offspring of triplo-X individuals. Am J Med Genet *18*, 357-364.

Nicklas, R.B and Jones, K. (1977). Chromosome distribution: Experiments on cell hybrids in vitro. Phil. Trans. R. Soc. London B. *277*, 267-276.

Phillips, C.M., and Dernburg, A.F. (2006). A family of zinc-finger proteins is required for chromosome-specific pairing and synapsis during meiosis in *C. elegans*. Dev. Cell *11*, 817-829.

Phillips, C.M., McDonald, K.L., and Dernburg, A.F. (2009). Cytological analysis of meiosis in Caenorhabditis elegans. Methods Mol. Biol. *558*, 171-195.

Phillips, C.M., Wong, C., Bhalla, N., Carlton, P.M., Weiser, P., Meneely, P.M., and Dernburg, A.F. (2005). HIM-8 binds to the X chromosome pairing center and mediates chromosome-specific meiotic synapsis. Cell *123*, 1051-1063.

852 Ratcliffe, S.G., Butler, G.E., and Jones. M. (1991). Edinburgh study of growth
853 and development of children with sex chromosome abnormalities. IV. in Children
854 and Young Adults With Sex Chromosome Aneuploidy. Ed. Evans, J.A, Hamerton,
855 J.L, Robinson, A. March of Dimes Birth Defects Foundation Birth efects Original
856 Article Series Vol. *26*, No.4, 1990.
857
858 Robinson, A., Bender, B.G., Linden, M.G., and Salbenblatt, J.A. (1991). Sex
859 chromosome aneuploidy: the Denver prospective study. in Children and Young
860 Adults With Sex Chromosome Aneuploidy. Ed. Evans, J.A, Hamerton, J.L,
861 Robinson, A. March of Dimes Birth Defects Foundation Birth efects Original
862 Article Series Vol. *26*, No.4, 1990.
863
864 Robles, P., Roig, I., Garcia, R., Ortega, A., Egozcue, J., Cabero, L.L. and Garcia,
865 M. (2007). Pairing and synapsis in oocytes from female fetuses with euploid and
866 aneuploid chromosome complements. Reproduction. 133: 899-907.
867
868 Roig, I., Robles, P., Garcia, R., Martínez-Flores, I., Cabero, L., Egozcue, J.,
869 Liebe, B., Scherthan, H., and Garcia, M. (2005). Chromosome 18 pairing
870 behavior in human trisomic oocytes. Presence of an extra chromosome extends
871 bouquet stage. Reproduction. *129*, 565-575.
872

873 Rogers, E., Bishop, J.D., Waddle, J.A., Schumacher, J.M., and Lin, R. (2002).
874 The aurora kinase AIR-2 functions in the release of chromosome cohesion in
875 *Caenorhabditis elegans* meiosis. J. Cell Biol. *157*, 219-229.
876
877 Schupbach, T, Wieschaus, E., and Nothinger, R. (1978). A study of the female
878 germline in mosaics of *Drosophila*. Wilhelm Roux's Archives *184*, 41-56.
879
880 Severson, A.F., and Meyer, B.J. (2014). Divergent kleisin subunits of cohesin
881 specify mechanisms to tether and release meiotic chromosomes.
882 Elife. 3:e03467.
883
884 Stewart, D.A., Bailey, J.D., Netley, C.T., and Park, E. (1991). Growth,
885 development, and behavioral outcome from mid-adolescence to adulthood in
886 subjects with chromosome aneuploidy: The Toronto study. in Children and
887 Young Adults With Sex Chromosome Aneuploidy. Ed. Evans, J.A, Hamerton, J.L,
888 Robinson, A. March of Dimes Birth Defects Foundation Birth efects Original
889 Article Series Vol. *26*, No.4, 1990.
890
891 Tada, T., Takagi, N., and Adler, I.D. (1993). Parental imprinting on the mouse X
892 chromosome: effects on the early development of X0, XXY and XXX embryos.
893 Genet. Res. *62*, 139-148.
894

Timmons, L., Court, D.L., and Fire, A. (2001). Ingestion of bacterially expressed dsRNAs can produce specific and potent genetic interference in *Caenorhabditis elegans*. Gene *263*, 103-112.

Wissmann, A., Ingles, J., Mains, P.E. (1999). The *Caenorhabditis elegans* mel-11 myosin phosphatase regulatory subunit affects tissue contraction in the somatic gonad and the embryonic epidermis and genetically interacts with the Rac signaling pathway. Dev Biol. 209: 111-127.

Yang, H.Y., McNally, K., and McNally, F.J. (2003). MEI-1/katanin is required for translocation of the meiosis I spindle to the oocyte cortex in *C. elegans*. Dev. Biol. *260*, 245-259.

Figure Legends

Figure 1. Trisomy correction during meiosis I. (A) Illustration showing expected outcomes of female meiosis in XXX wild-type worms assuming the extra univalent X (red) does not lose cohesion (yellow) between sister chromatids during anaphase I, and assuming random segregation. (B) Illustration of a spindle with chromosomes at the metaphase plate with poles marked "P" (left) and a projection of the cross-sectional view down the pole to pole axis at the metaphase plate (right). (C-E) Z projections of fixed meiotic embryos viewed down the pole to pole spindle axis. Meiotic embryos from XXX wild-type mothers were stained with DAPI and anti-tubulin antibody. (C) Metaphase I spindles with 7 chromosomes; right images of X-FISH show two X chromosomes on the spindle. See also Supplemental Stack 1. (D) Metaphase II spindles with 6 chromosomes; right images of X-FISH show one X on the spindle and 2-3 foci in the polar body. See also supplemental Stack 2. (E) Metaphase II spindle with 7 chromosomes. (F) Frequency of each spindle class among the progeny of XXX wild-type mothers. Insets show polar bodies, marked by asterisks, which were used to identify metaphase II spindles. Bar = 5 μm.

Figure 2. X univalents are preferentially lost between metaphase I and metaphase II in *him-8* mutants. Z projections of living (A-E) and fixed (F-J) C. elegans meiotic embryos viewed down the pole to pole spindle axis at metaphase I (A ,B, F, G) or metaphase II (C, D, E, H, I, J). mCherry::Histone H2B and GFP::tubulin label the chromosomes and spindle respectively in live

embryos. Fixed embryos were stained with DAPI, anti-tubulin antibody and a LacO FISH probe that recognizes a LacO array integrated on the X chromosome. Asterisks indicate polar bodies. Insets show polar bodies that did not fit in the image frame. In (E) “s” denotes a sperm outside of the embryo. Percentages are shown for each outcome (K, L). Bar = 5 μm.

Figure 2- figure supplement 1. *zim-2* embryos also deposit unpaired chromosome V univalents into the first polar body. Z projections of fixed meiotic embryos viewed down the pole to pole spindle axis. Embryos were stained with DAPI, anti-tubulin antibody and a LacO FISH probe that recognizes a LacO array integrated on chromosome V. This array is larger than the array inserted on X thus the foci are larger than those shown in Fig. 2. (A) Metaphase I embryo with 7 DAPI chromosomes and two LacO (V) univalents. (B) Metaphase II embryo with 5 DAPI chromosomes and no LacO (V) chromosome on the spindle and two in the first polar body. (C) Metaphase II embryo with 6 DAPI chromosomes and one LacO (V) chromosome on the spindle and one in the first polar body. (D) Early anaphase II spindle with 2 LacO (V) chromosomes in the spindle and none in the first polar body. In B and C polar bodies are marked by asterisks. In D the polar body is shown as an inset because it was in a distant focal plane. (E) Quantification of the frequencies of each class. (F) Diakinesis chromosome counts from the *zim-2* and *him-8* strains bearing Lac operator arrays. Left panel shows representative *zim-2* diakinesis nucleus with 6

957 chromosomes, right two panels show two examples of *zim-2* diakinesis nuclei
958 with 7 chromosomes. Bar = 5 μm.

959

960 **Figure 3. X univalents biorient at metaphase I in *him-8* embryos.** (A)
961 Cartoon diagram of REC-8 staining on bivalents and univalents. (B and C) Anti-
962 REC-8 staining of metaphase I and metaphase II embryos with bivalents (yellow
963 arrow head) and univalents (white arrow head). In *him-8* embryos, univalents at
964 metaphase I have a single band of REC-8 with the same orientation seen on
965 normal chromosomes at metaphase II. (D) Quantification of the orientation of
966 univalents, by offset angle from the metaphase plate, 0° corresponds to perfect
967 biorientation and 90° corresponds to perfect mono-orientation. Cortical pole is on
968 the left in all images. Bar = 5 μm.

969

970 **Figure 3- figure supplement 1. Imaging of GFP::KNL-2 demonstrates that**
971 ***him-8* univalent chromosomes biorient at metaphase of meiosis I.** (A-B) Z-
972 projections through fixed GFP::KNL-2 embryos stained with DAPI and anti-
973 tubulin antibody. (A) Metaphase I wild type and *him-8* embryos showing the
974 distinct KNL-2 cups around bivalents (yellow arrow head) and univalents (white
975 arrow head). (B) Metaphase II wild type and him-8 embryos showing the
976 characteristic KNL-2 cups around bioriented chromosomes at the metaphase
977 plate. (C) Quantification of the orientation of chromosomes, by offset angle from
978 the metaphase plate, 0° corresponds to perfect biorientation and 90°

corresponds to perfect mono-orientation. Cortical pole is on the left in all images. Bar = 5 μm.

Figure 3- figure supplement 2. Reduced levels of AIR-2 are loaded on *him-8* X univalents at meiosis I. (A and B) Z projections of fixed metaphase I, GFP:AIR-2 embryos stained with DAPI and anti-tubulin antibody. AIR-2 is loaded between homologs of both wild-type (A) and *him-8* bivalents (B) whereas less AIR-2 was observed on *him-8* univalents (arrow heads in B). (C) Relative pixel intensity ratios show that *him-8* metaphase II chromosomes load 1.7 times as much AIR-2 as X univalents at metaphase I, and metaphase I bivalents load 2.3 times as much AIR-2 as X univalents at metaphase I. n for both refers to total number of embryos counted, where each metaphase II embryo bore 5-7 chromosomes, and each metaphase I embryo bore 2 univalents and 5 bivalents. Bar = 5 μm.

Figure 4. X univalents lag at anaphase I. (A) Time-lapse images of a living wild-type embryo undergoing anaphase I show chromosomes separating as two distinct masses. (B) Time-lapse images of a living *him-8* embryo show a lagging chromosome at anaphase I. (C - E) Z projections of fixed anaphase I embryos. (C) LacO FISH labeling of a wild-type strain with a LacO array integrated on the X chromosome shows normal segregation of two X homologs from one X

bivalent. (D) LacO FISH shows that a lagging chromosome in *him-8* is the X. (E) LacO FISH labeling of a *zim-2* strain with a LacO array integrated on chromosome V showing a univalent V lagging at anaphase I. Cortical pole is to the left in all images. Bar = 5 μm.

Figure 5. The contractile ring moves inward past the lagging chromosomes of *him-8* embryos. (A) Time-lapse sequence of anaphase I in a *him-8* strain with GFP::PH, GFP::Tubulin and mCherry::Histone H2B. The plasma membrane ingresses past the lagging chromosomes to engulf them in the polar body. (B) Fraction of *him-8* anaphase I embryos in which a lagging chromosome eventually resolved toward the cortex or eventually resolved into the embryo (interior). Lagging univalents resolved more frequently toward the cortex during both early and late anaphase. Depletion of NMY-2, the myosin required for polar body formation, eliminated only the late anaphase bias. Pairwise two tailed p values by Fisher's exact test: *him-8* late vs *him-8 nmy-2(RNAi)* late = .02, *him-8* early vs *him-8 nmy-2(RNAi)* early = .80, *him-8* early vs *him-8* late = 1.0, *him-8 nmy-2(RNAi)* early vs *him-8 nmy-2(RNAi)* late = .26. p values from Pearson's Chi Squared test: *him-8* late vs 50% = .003, *him-8 nmy-2(RNAi)* late vs 50% = .32, *him-8* early vs 50% = .02, *him-8 nmy-2(RNAi)* early vs 50% = .38. (C) Top, diagram illustrating how the position of scission by the contractile ring along the pole to pole spindle axis was scored. Bottom, representative images from time-lapse sequences showing scission at different positions along the length of the spindle. (D) Average position of contractile ring scission along the pole to pole

spindle axis in wild-type embryos and in *him-8* embryos with no lagging chromosomes, lagging chromosomes that end up at the cortex (Cortical), or lagging chromosomes that end up in the embryo (Interior). Bar = 5 μm.

Figure 6. Lagging chromosomes are captured by the septin tube and expelled with polar bodies. Time-lapse imaging of embryos expressing GFP::septin and mCherry::histone. (A) Time-lapse images of a living wild-type embryo undergoing anaphase I show the conversion of a flat washer-shaped contractile ring into a tube during formation of the first polar body. (B) Time-lapse images of a living *him-8* embryo show two lagging chromosomes at anaphase I (arrows) as one moves into the polar body early on, while the second is trapped in the septin tube and is extruded with the first polar body. (C) Two time points of a *him-8* embryo during telophase I showing the lagging chromosome trapped in the septin tube. Bar = 4 μm. Times are from the onset of homolog separation.

Figure 7. Early bias of univalent X chromosomes might occur at the metaphase to anaphase I transition. Representative cartoon diagrams and Z projections from fixed embryos stained with DAPI, anti-tubulin antibody, and LacO(X) FISH probe. Cortex is at the top. (A-C) Both X univalents on metaphase I spindles that were shortened (5.3 - 7.2 μm spindle length) but still parallel to the embryo cortex were frequently (46%) aligned closer to the same spindle pole. (D-

1046 F) One or both univalents on MI spindles that had rotated but homologs had not
1047 yet separated were closer to the cortex and future polar body in 38 + 19% of
1048 embryos. Both univalents were never observed closer to the interior spindle
1049 pole. Yellow dashed lines indicate the metaphase plate. (H and I) Time-lapse
1050 images of two univalents (arrows in H) or one univalent (arrowhead in I) offset
1051 from the metaphase plate just before rotation of the univalent-proximal pole to
1052 the cortex. Time zero is initiation of spindle rotation. Bar = 5 μm.

1053

1054

Table 1. Enhancement of the segregation bias in *him-8* mutants by mutations in the myosin phosphatase, *mel-11*

Self progeny counts

genotype	temperature (°C)	% XO male	% XX hermaphrodite	% XXX Dpy	total progeny
mel-11(sb55) unc-4	20	0.2	99.8	NC	1763
mel-11(sb55) unc-4; him-8	20	49*	51	NC	374
unc-4; him-8	20	34	66	NC	1442
mel-11(it126) unc-4	15	0.6	99	NC	790
mel-11(it126) unc-4; him-8	15	58*	38.6	3.4	873

Ratio of nulloX ova/diploX ova calculated from progeny of cross with *lon-2* males

maternal genotype	temperature (°C)	# nulloX (lon male progeny)	# diploX (dpy progeny)	nullo/diplo	total progeny
mel-11(it26) unc-4	25	1	0	NA	785
mel-11(it26) unc-4; him-8	25	160	7	22.9	595
unc-4; him-8	25	98	31	3.2	677

Table 1. *mel-11* increases the frequency of male progeny from *him-8* mothers. *mel-11(sb55)* and *mel-11(it26)* worms produce high frequencies of dead embryos which cannot be scored for sex at 25°C (Wissman et al., 1999). Percent male (XO), hermaphrodite (XX) and dumpy (XXX) progeny from self-fertilizing *mel-11*, *him-8* or *him-8 mel-11* double mutant worms were therefore scored at 15°C and 20°C. Only progeny that developed to the L4 or adult stage were counted. * two tailed p<.0001 by binomial test compared with *him-8* alone. 100% of *mel-11(it26)* self progeny die as embryos at 25°C but this lethality is rescued by *mel-11(+)* sperm (Kemphues et al., 1988). The progeny of *mel-11(it26)* hermaphrodites crossed with *lon-2* males could therefore be scored at 25°C. When *lon-2(+)* hermaphrodites are crossed with *lon-2* males (*lon-2* is a recessive X-linked marker), 50% of the ova will be fertilized by sperm with a single *lon-2* X chromosome. Fertilization of a nullo X ova by a a *lon-2* X sperm will result in a *lon-2* male. Fertilization of a diploX ova by a *lon-2* X sperm will result in a XXX dumpy worm. Random segregation of the unpaired X chromosomes in *him-8* would result in a ratio of nullo X/diplo X ova of 1.0. The *mel-11; him-8* double mutant showed a 7-fold increase in the ratio of nullo/diploX ova relative to *him-8* alone, indicating an increased efficiency of eliminating maternal unpaired X chromosomes.

List of Supplemental Material

Supplementary File 1: *C. elegans* strains used in this study

Supplementary File 2. Z-stack of XC FISH on XXX wild-type metaphase plate in meiosis I. 16 bit 3 channel TIFF can be opened using FIJI or basic ImageJ (http://fiji.sc/Downloads). Data shown is a z-stack acquired with 300nm steps through a meiosis I metaphase spindle. Chromosomes are shown in blue (DAPI), tubulin antibodies label the spindle in green, and the XC FISH probe labels X chromosomes (2 present) in red. Channels can be split for individual analysis using the channel splitter (Image>Colors>Split Channels) or can be hidden using the channels tool (Image>Colors>Channels Tool).

Supplementary File 3. Z-stack of XC FISH on XXX wild-type metaphase plate in meiosis II. 16 bit 3 channel TIFF can be opened using FIJI or basic ImageJ (http://fiji.sc/Downloads). Data shown is a z-stack acquired with 300nm steps through a meiosis II metaphase spindle. Chromosomes and the first polar body, which is on the top, are shown in blue (DAPI), tubulin antibodies label the spindle in green, and the XC FISH probe labels X chromosomes (1 present on the spindle) in red. Channels can be split for individual analysis using the channel splitter (Image>Colors>Split Channels) or can be hidden using the channels tool (Image>Colors>Channels Tool).

Figure 1

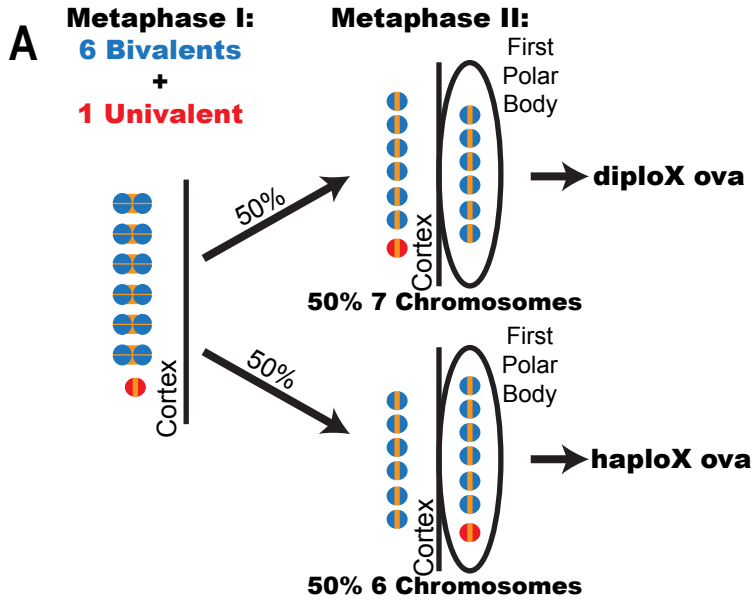

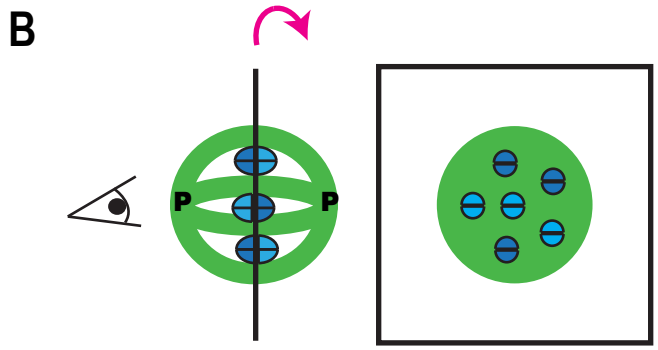

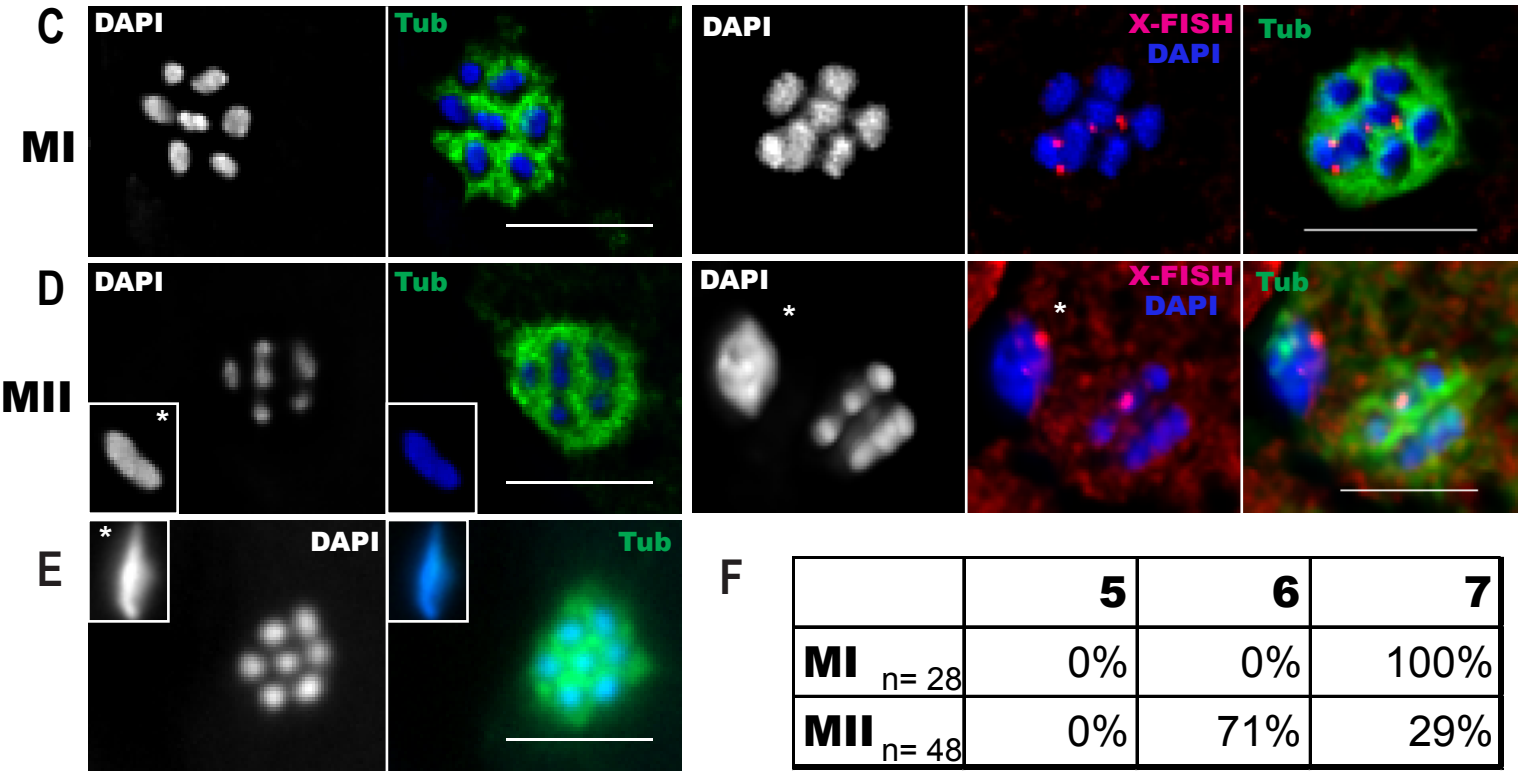

F

	5	6	7
MI n= 28	0%	0%	100%
MII n= 48	0%	71%	29%

Figure 2

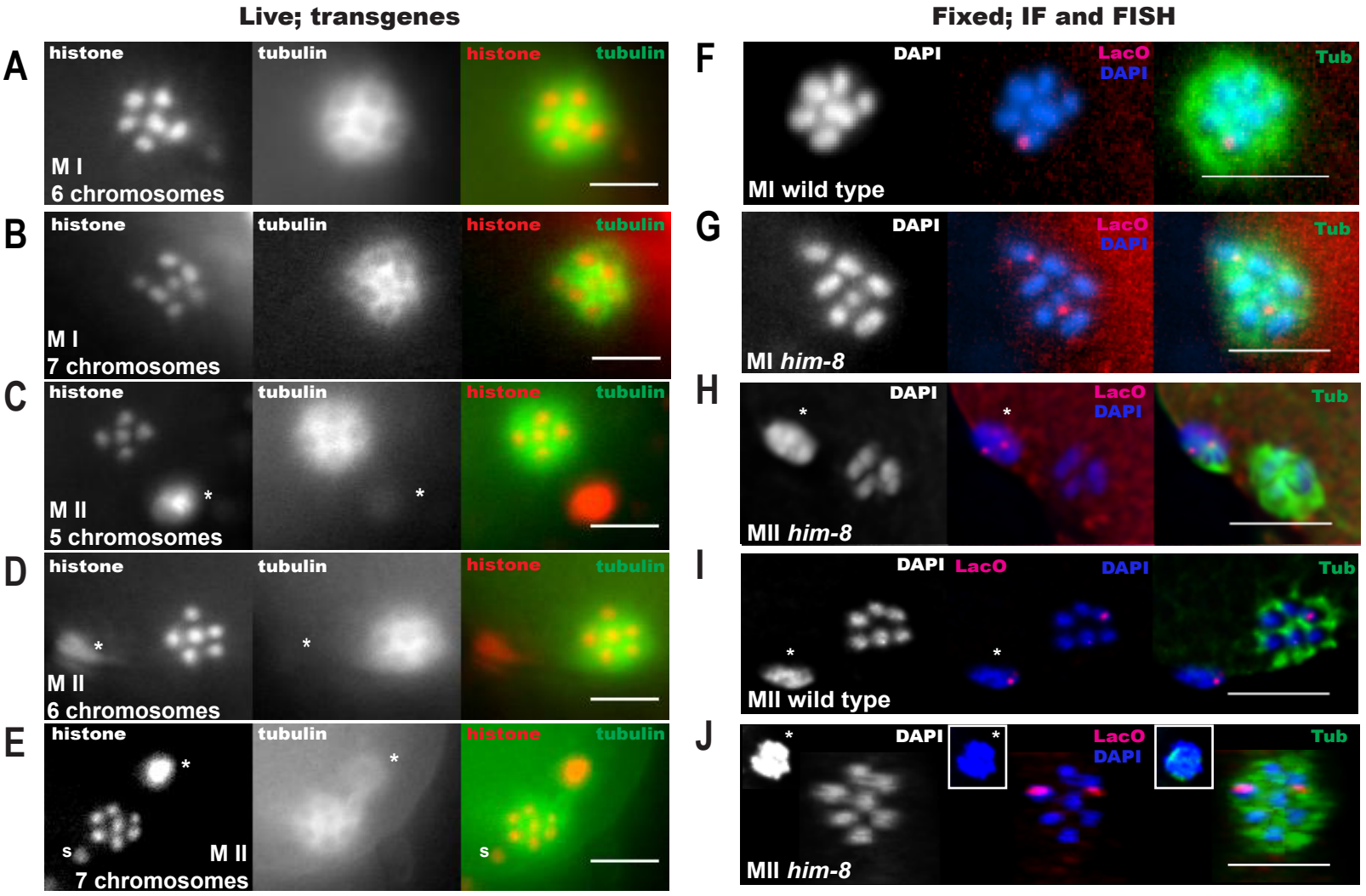

K

MI	chromosome #	5	6	7
	WT n=21	0	100%	0
	him-8 n=51	0	4%	96%
MII	**WT** n=33	0	100%	0
	him-8 n=87	40%	55%	5%

L

MI	chromosome #	5	6	7
	WT n=50	0	100%	0
	him-8 n=69	0	7%	93%
MII	**WT** n=29	0	100%	0
	him-8 n=110	38%	55%	7%

Figure 3

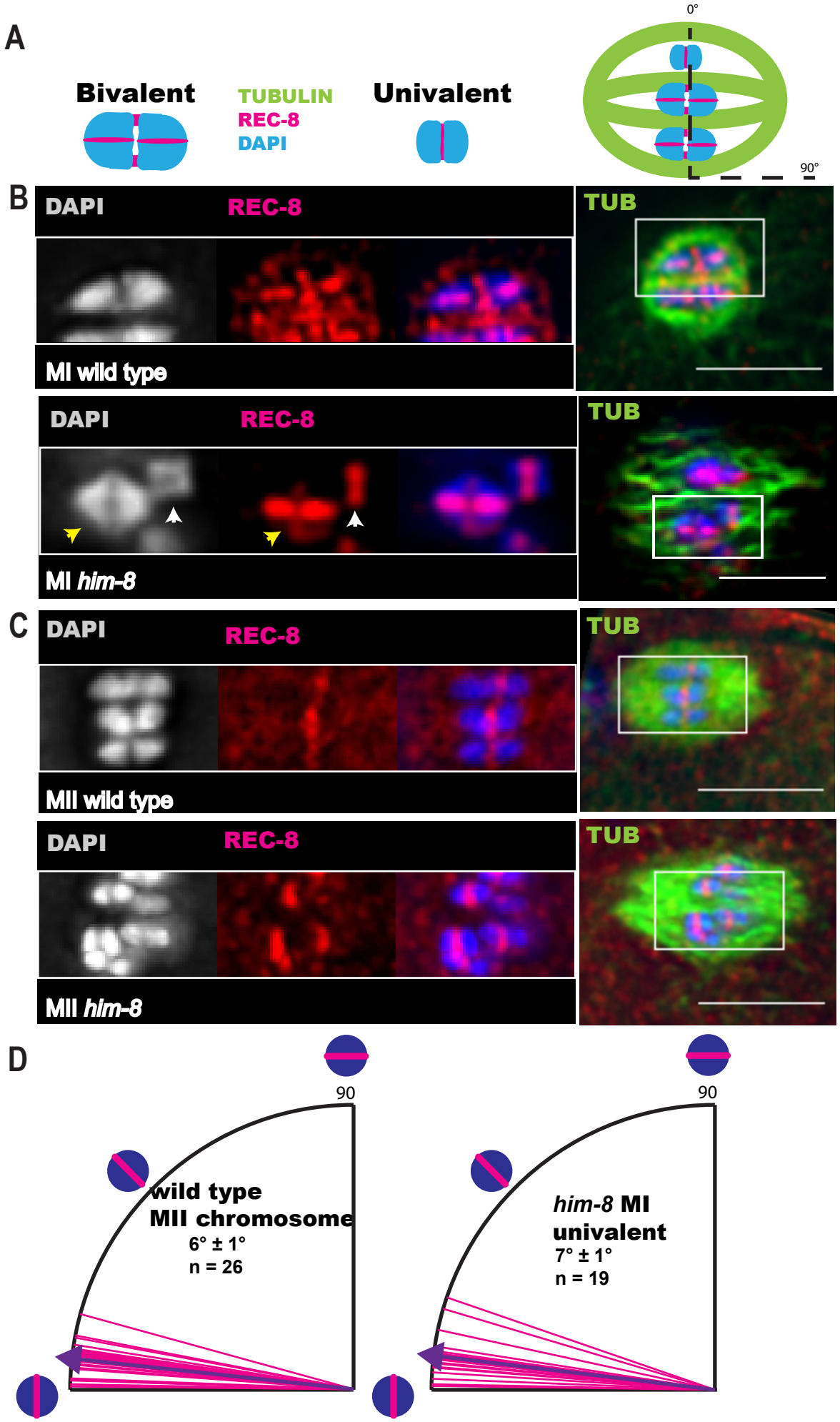
A
Bivalent
TUBULIN
REC-8
DAPI
Univalent
0°
90°
B
DAPI
REC-8
TUB
MI wild type
DAPI
REC-8
TUB
MI him-8
C
DAPI
REC-8
TUB
MII wild type
DAPI
REC-8
TUB
MII him-8
D
90
wild type
MII chromosome
6° ± 1°
n = 26
90
him-8 MI
univalent
7° ± 1°
n = 19

Figure 4

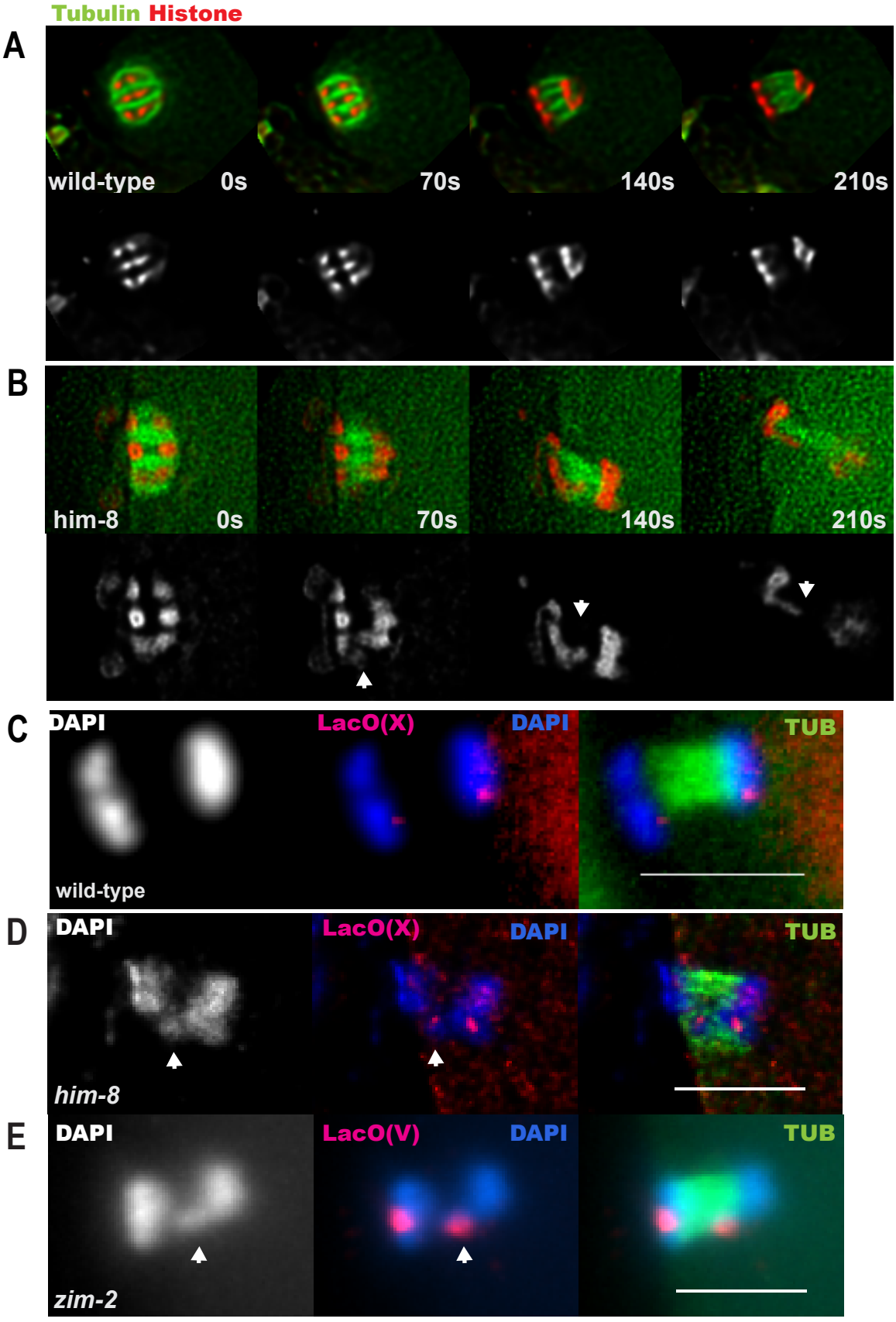
Tubulin Histone
A
wild-type
0s
70s
140s
210s
B
him-8
0s
70s
140s
210s
C
DAPI
LacO(X)
DAPI
TUB
wild-type
D
DAPI
LacO(X)
DAPI
TUB
him-8
E
DAPI
LacO(V)
DAPI
TUB
zim-2

Figure 5

A

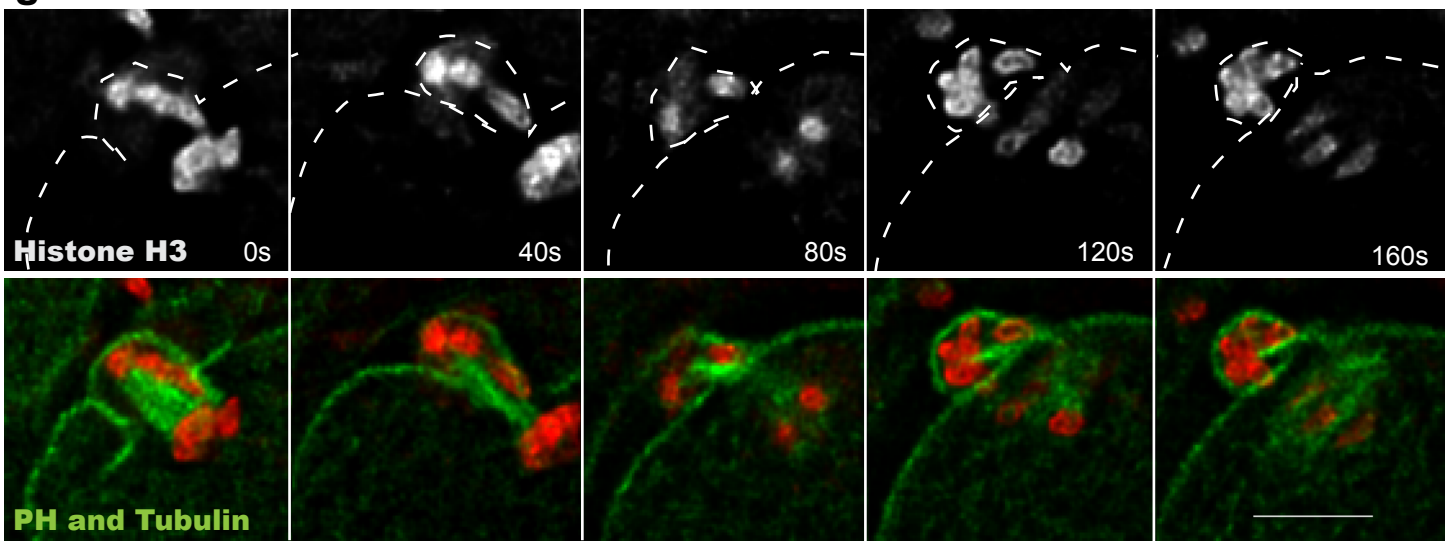

B

Contractile ring-dependent resolution bias of lagging chromosomes at anaphase I

	Early Resolving			Late Resolving		
	Cortical	Interior	n	Cortical	Interior	n
***him-8* control**	64%	36%	72	64%	36%	109
him-8 nmy-2(RNAi)	60%	40%	20	42%	58%	36

C

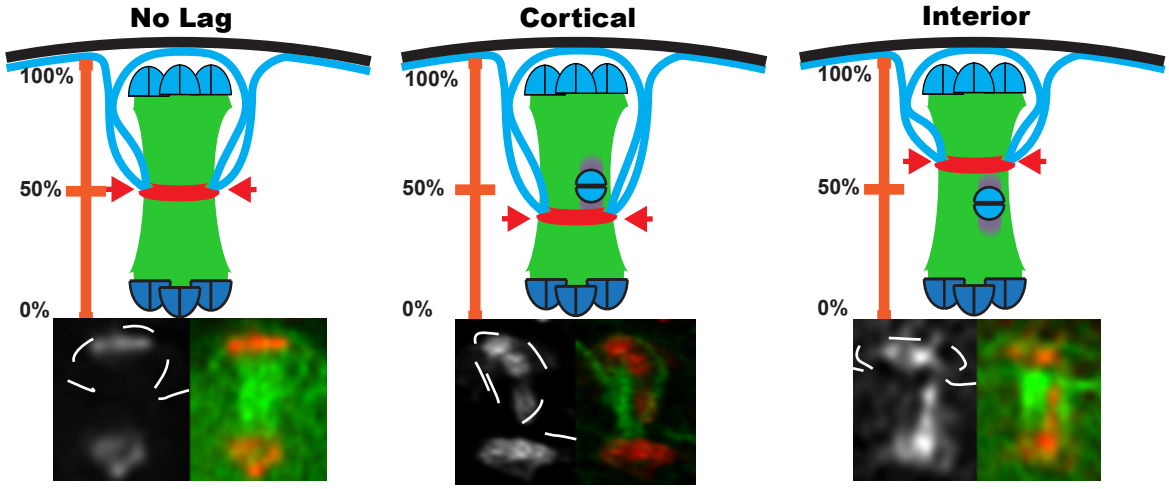

D

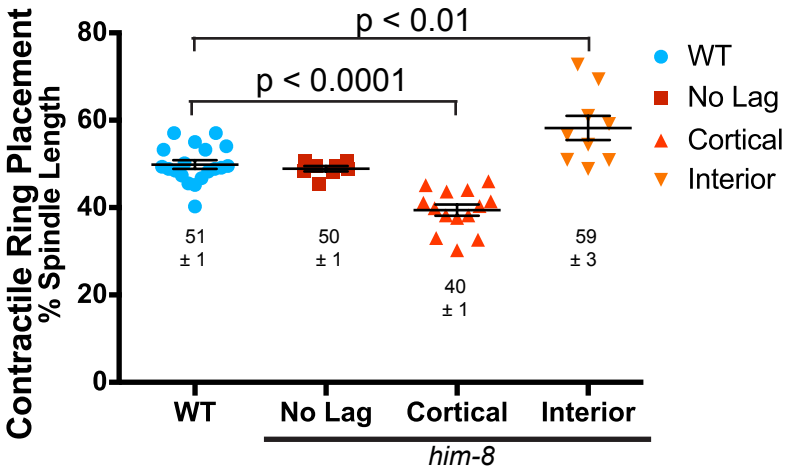

Figure 6

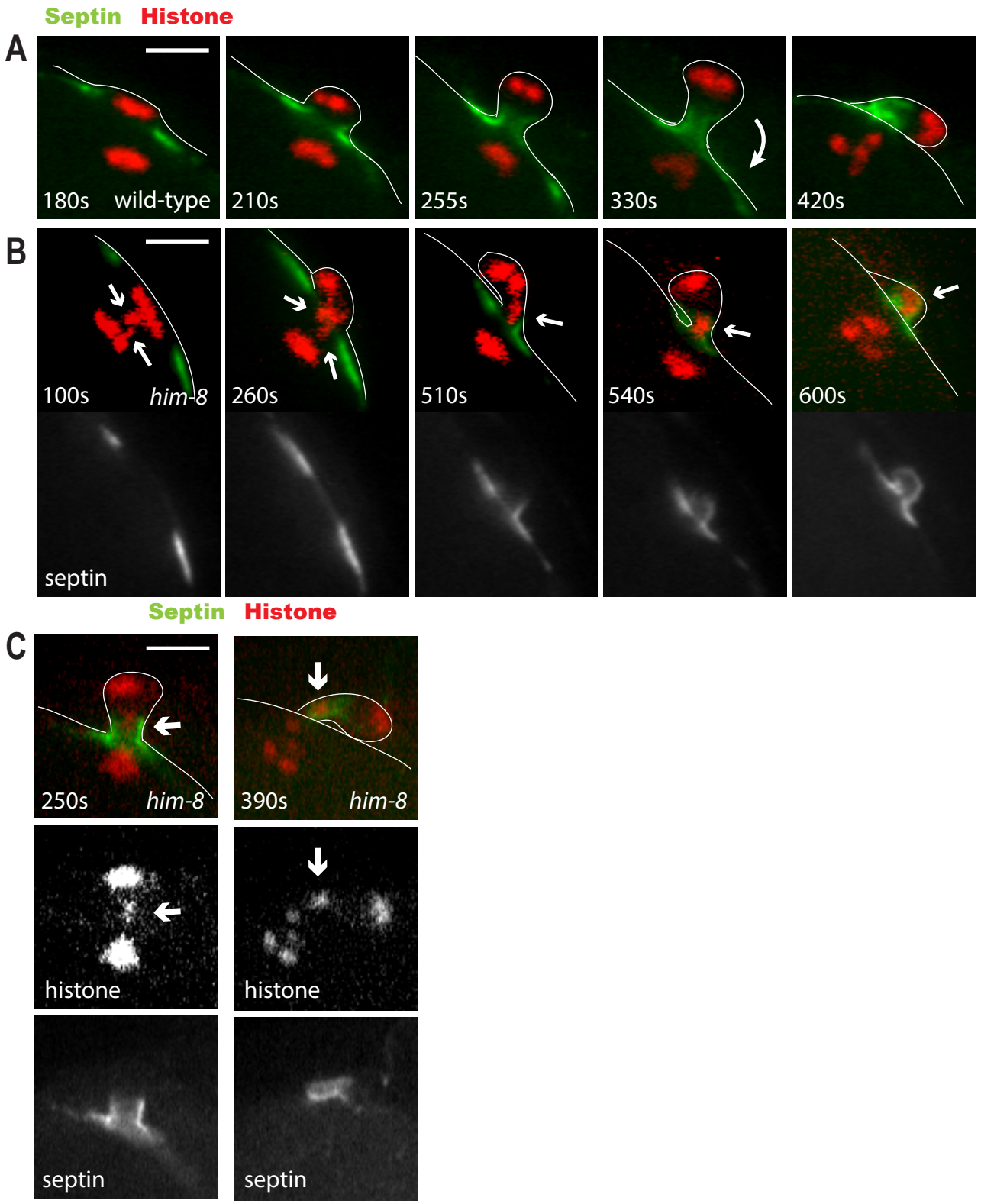
Septin Histone
A
180s wild-type
210s
255s
330s
420s
B
100s him-8
260s
510s
540s
600s
septin
Septin Histone
C
250s him-8
390s him-8
histone
histone
septin
septin

Figure 7

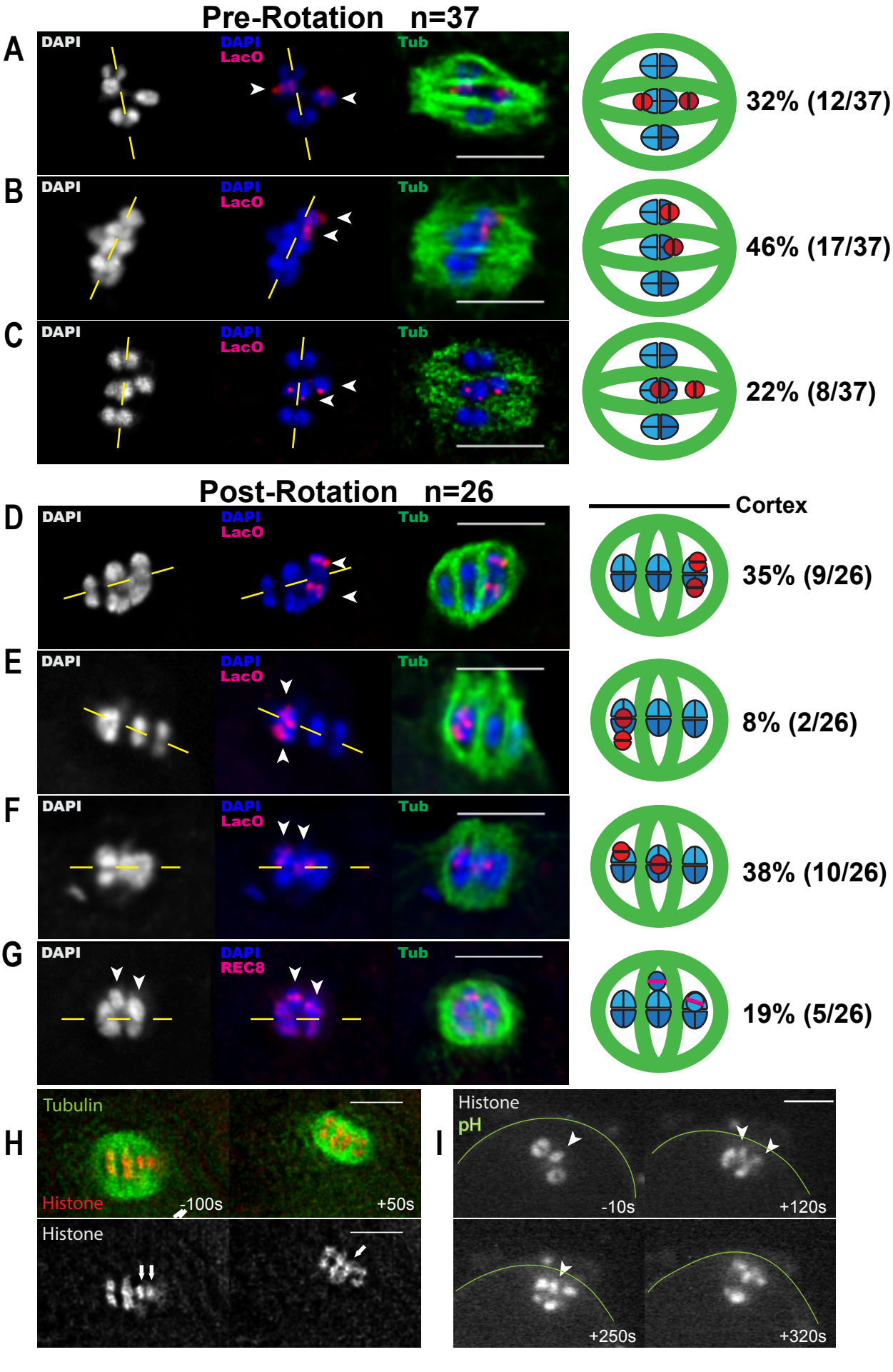
Pre-Rotation n=37
A
B
C
DAPI
DAPI
LacO
Tub
32% (12/37)
46% (17/37)
22% (8/37)
Post-Rotation n=26
D
E
F
G
DAPI
REC8
Cortex
35% (9/26)
8% (2/26)
38% (10/26)
19% (5/26)
H
Tubulin
Histone
-100s
+50s
I
pH
-10s
+120s
+250s
+320s